PLANT GENETICS

A tripartite genetic conflict system controls hybrid sterility in rice

Xiaodong He[1]†, Zhigang Zhao[1]†, Kun Shao[1]†, Xiaowen Yu[1]†, Ying Zhu[3]†, Jintao Tang[4]†, Jing Li[5], Yunhui Zhang[1], Keyu Zhao[1], Xiaoming Zheng[2], Hongru Wang[6], Chao Li[1], Xiangchao Gan[1], Xiaoou Dong[1], Yulong Ren[2], Yehui Xiong[2], Jian Wang[2], Yang Hu[1], Siqi Cheng[1], Bowen Yao[1], Yulu Ye[6], Song Guo[1], Yuantao Zhu[1], Ling He[1], Tiaofeng Shan[1], Chen Xu[1], Jinxuan Xu[1], Jiayu Lu[1], Dekun Lei[1], Anqi Jian[1], Junwen Gao[1], Song Cui[1], Gencheng Xu[1], Xiuping Guo[2], Xi Liu[1], Yunlu Tian[1], Shijia Liu[1], Ling Jiang[1], Xianneng Deng[5], Jiawu Zhou[5], Dayun Tao[5], Yonglun Zeng[3,7], Letian Chen[4]*, Chuanyin Wu[2]*, Haiyang Wang[2]*, Chaolong Wang[1,2]*, Jianmin Wan[1,2]*

Interspecific Asian–African hybrid rice could substantially boost yield but is limited by severe hybrid sterility. We identify *RHS3* as a major quantitative trait locus controlling this trait. *RHS3* encodes a tripartite toxin–antidote system composed of MAO, DUN, and JIA, in which MAO acts as a toxin that aborts gametes by disrupting mitochondrial function, whereas DUN and JIA function as antidotes that neutralize MAO toxicity, conferring a transmission advantage to the African allele. We demonstrate that detoxification relies on selective autophagy through formation of a tripartite JIA–DUN–MAO protein complex. We infer the de novo origin of *RHS3* in the AA-genome rice lineage, illustrating a role for genetic conflict in speciation and suggesting strategies to harness heterosis between Asian and African rice.

Rice (*Oryza sativa*) is the staple food for more than half of the world's population and is central to global food security (*1*, *2*). Only two rice species have been domesticated: Asian rice (*O. sativa* L.), derived from *O. rufipogon* in Asia, and African rice (*O. glaberrima* Steud.), derived from *O. barthii* in West Africa (*3*–*6*). Asian rice is characterized by high yield and grain quality, whereas African rice possesses strong tolerance to biotic and abiotic stresses (*7*, *8*). Consequently, interspecific Asian–African hybrid rice can outperform conventional rice varieties by 30 to 60%, offering substantial potential to increase rice productivity (*9*, *10*). However, severe postzygotic reproductive isolation, particularly hybrid sterility, limits the effective exploitation of this interspecific heterosis (*11*). Despite extensive efforts to elucidate the genetic basis of hybrid sterility between the two species, only one locus, *S1*, has been cloned, and its underlying molecular mechanism remains unresolved (*12*, *13*). Thus, how hybrid sterility loci establish reproductive isolation between rice species remains largely unknown, posing a major barrier to the utilization of the interspecific heterosis between Asian and African rice.

Hybrid sterility is often caused by incompatible allelic interactions at specific loci, many of which encode toxin–antidote systems (also known as meiotic drivers or segregation distorters) in diverse plant and animal species (*14*–*17*). Well-known examples include the *PK3* locus in *Arabidopsis* (*18*), the *S5*, *qHMS7*, and *RHS12* loci in rice (*19*–*21*), the *sup-35/pha-1* elements in nematodes (*22*), and the *t*-complex in mice (*23*). In hybrids, incompatible allelic interactions at these loci provoke genetic conflict, conferring a transmission advantage on carrier alleles over noncarriers and thereby distorting Mendelian inheritance. Such transmission advantages can promote the spread of carrier alleles within natural populations, contributing to speciation and maintenance of species boundaries (*24*–*26*). Despite the prevalence of hybrid sterility loci across diverse taxa, their evolutionary origins and molecular mechanisms remain poorly understood, limiting our understanding of the forces that drive speciation.

Here, we identified and cloned *RHS3*, a major locus underlying hybrid sterility between Asian and African cultivated rice. Functional and evolutionary analyses revealed a noncanonical tripartite toxin–antidote system and uncovered a direct mechanistic link between selective autophagy and reproductive isolation. These findings provide insights into the evolution of interspecific genetic conflict and offer a genetic framework for overcoming reproductive barriers and exploiting interspecific heterosis between Asian and African rice.

RHS3 controls interspecific hybrid sterility

Hybrids between Asian and African cultivated rice displayed severe hybrid sterility, with markedly reduced pollen and spikelet fertility (Fig. 1A). Quantitative trait loci mapping in a BC_1F_1 population derived from DJY1 (Dianjingyou1, a *japonica* variety of Asian cultivated rice, genotype *jj*) and IRGC 102295 (an African cultivated rice accession, genotype *gg*) identified two rice hybrid sterility ("RHS") loci on chromosomes 3 and 7, designated *RHS3* and *RHS7* (fig. S1A and data S3). Because *RHS3* colocalized with the previously reported *S19*/*S64* region associated with interspecific hybrid sterility (*27*, *28*), we prioritized it for further analysis.

A near-isogenic line (NIL) carrying the IRGC 102295 allele at *RHS3* (NIL-*RHS3*) was developed in the DJY1 background (fig. S1B). DJY1 (*RHS3-jj*), NIL-*RHS3* (*RHS3-gg*), and their F_1 hybrids (F_1-*RHS3*, *RHS3-gj*) developed normally and showed high spikelet fertility (Fig. 1A and fig. S1C). By contrast, F_1-*RHS3* plants displayed pollen semisterility, whereas both parental lines exhibited >95% pollen fertility (Fig. 1A). Cytological analyses revealed no obvious defects during tapetum degeneration or early microspore development, but nearly half of the pollen grains showed delayed development at the polarized microspore stage and were arrested at the bicellular stage, exhibiting reduced starch accumulation and defective pollen wall formation (fig. S1, D and E).

Reciprocal crosses revealed that *RHS3-gj* and *RHS3-jj* progeny segregated at a 1:1 ratio when F_1-*RHS3* served as the female parent and DJY1 as the male parent, whereas only *RHS3-gj* progeny were recovered when F_1-*RHS3* was used as the pollen donor (Fig. 1B), indicating normal female fertility and transmission failure of *RHS3-j* pollen. Consistent with this observation, F_1-*RHS3* plants displayed pollen semisterility irrespective of cytoplasmic background, and the F_2 population segregated 1:1 into fertile (*RHS3-gg*) and semisterile (*RHS3-gj*) plants (fig. S2). Together, these results establish *RHS3* as a single nuclear gamete-killer locus that selectively eliminates *RHS3-j* pollen.

To identify the gene(s) underlying *RHS3*, we compared the corresponding genomic intervals in DJY1 and IRGC 102295. The *RHS3* locus spans 53.8 kb in DJY1 and 142.7 kb in IRGC 102295, largely owing to a ~94.3-kb structural variant (SV) in the latter. Seventeen open reading frames (ORFs) were predicted within the aligned interval, including nine shared genes, one DJY1-specific gene, and seven IRGC 102295-specific genes (Fig. 1C and data S4).

[1]State Key Laboratory for Crop Genetics & Germplasm Enhancement and Utilization, Zhongshan Biological Breeding Laboratory, National Observation and Research Station of Rice Germplasm Resources, Nanjing Agricultural University, Nanjing, China. [2]State Key Laboratory for Crop Gene Resources and Breeding, Institute of Crop Sciences, Chinese Academy of Agricultural Sciences, Beijing, China. [3]State Key Laboratory of Plant Diversity and Specialty Crops and Guangdong Provincial Key Laboratory of Applied Botany, South China Botanical Garden, Chinese Academy of Sciences, Guangzhou, China. [4]Guangdong Laboratory for Lingnan Modern Agriculture, Guangdong Basic Research Center of Excellence for Precise Breeding of Future Crops, College of Agriculture, South China Agricultural University, Guangzhou, China. [5]Yunnan Seed Laboratory, Yunnan Key Laboratory for Rice Genetic Improvement, Food Crops Research Institute, Yunnan Academy of Agricultural Sciences, Kunming, China. [6]Agricultural Genomics Institute at Shenzhen, Chinese Academy of Agricultural Sciences, Shenzhen, China. [7]University of Chinese Academy of Sciences, Beijing, China. ***Corresponding author. Email: wanjianmin@caas.cn (J.Wan), wcl@njau.edu.cn (C.Wang), wanghaiyang@caas.cn (Haiyang Wang), wuchuanyin@caas.cn (C.Wu), lotichen@scau.edu.cn (L.C.)** †These authors contributed equally to this work.

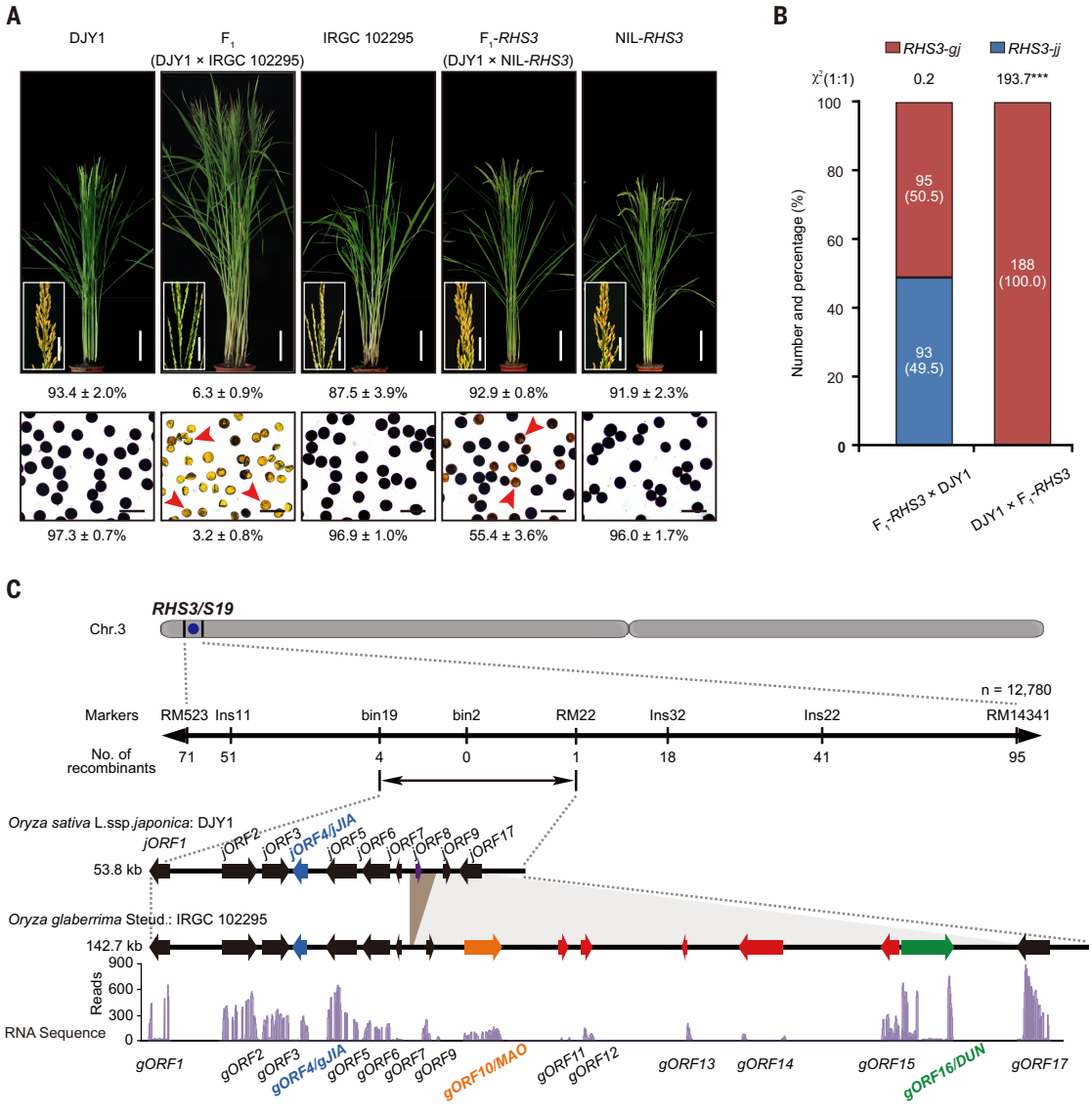

Fig. 1. Genetic analysis and cloning of *RHS3*. (**A**) Representative plant morphology (top), with spikelet fertility shown as insets, and pollen viability (bottom) of Asian rice DJY1, African rice IRGC 102295, near-isogenic line NIL-*RHS3*, and their F_1 hybrids (DJY1 × IRGC 102295; DJY1 × NIL-*RHS3*, named F_1-*RHS3*) ($n = 5$ independent florets or panicles). Red arrowheads indicate aborted pollen grains. Scales bars: 20 cm (plant), 5 cm (panicle), 100 μm (pollen). (**B**) Genotypic distribution of *RHS3-gj* or *RHS3-jj* alleles in progeny from reciprocal crosses between DJY1 and F_1-*RHS3*. Percentages and total plant numbers are shown for each cross direction. Asterisks indicate statistically significant differences (χ^2 test, $^{***}P < 0.001$). (**C**) Genomic organization of the *RHS3* locus. A total of 17 ORFs are annotated within the mapped interval. *ORF4* encodes JIA, *gORF10* encodes MAO, and *gORF16* encodes DUN.

MAO–DUN encodes a toxin–antidote system

The selective elimination of *RHS3-j* pollen in F_1-*RHS3* plants suggest that the *RHS3-g* region from African cultivated rice harbors a toxin–antidote system. Individual disruption of the 16 predicted genes within this region in F_1-*RHS3* plants revealed that pollen viability was restored only by knocking out *gORF10* (Fig. 2A and data S5). Consistent with this, genotypic segregation at *RHS3* in T_1 progeny reverted to the expected Mendelian 1:2:1 ratio (*jj:gj:gg*) (Fig. 2B and fig. S3, A and B), demonstrating that *gORF10* functions as the toxin that eliminates *RHS3-j* pollen. We therefore named this gene *MAO*, meaning "spear" in Chinese.

By contrast, repeated attempts failed to disrupt *gORF16* in F_1-*RHS3*-derived calli, suggesting that it functions as an antidote in pollen as well as somatic cells. Using green fluorescent protein (GFP) as a proxy for cell viability, we found that *MAO* expression abolished GFP signal in rice calli, whereas coexpression of *gORF16* restored the signal (fig. S3, C and D). Consistent with this, knocking out *gORF16* in the *MAO* mutant background generated *MAO/gORF16* double mutants with normal pollen and spikelet fertility (fig. S3, E to G). Moreover, introduction of a genomic copy of *gORF16* into F_1-*RHS3* plants increased pollen viability to approximately 75% in T_0 transformants (Fig. 2C), and segregation at both the *RHS3* and transgene loci in T_1 progeny followed the expected 1:3:2 ratio (*RHS3, jj:gj:gg*; transgene, *–:t-:tt*) (Fig. 2D and fig. S4, A to C). Together, these findings suggest that *gORF16* acts as the antidote that restores fertility to *RHS3-j* pollen. We therefore named this gene *DUN*, meaning "shield" in Chinese.

Introduction of linked *MAO* and *DUN* transgenes into DJY1 recapitulated the F_1-*RHS3* phenotype, causing pollen semisterility without affecting spikelet fertility (fig. S4, D to F). The transgene likewise segregated in a 0:1:1 ratio (*–:t-:tt*) in T_1 progeny (fig. S4, G and H),

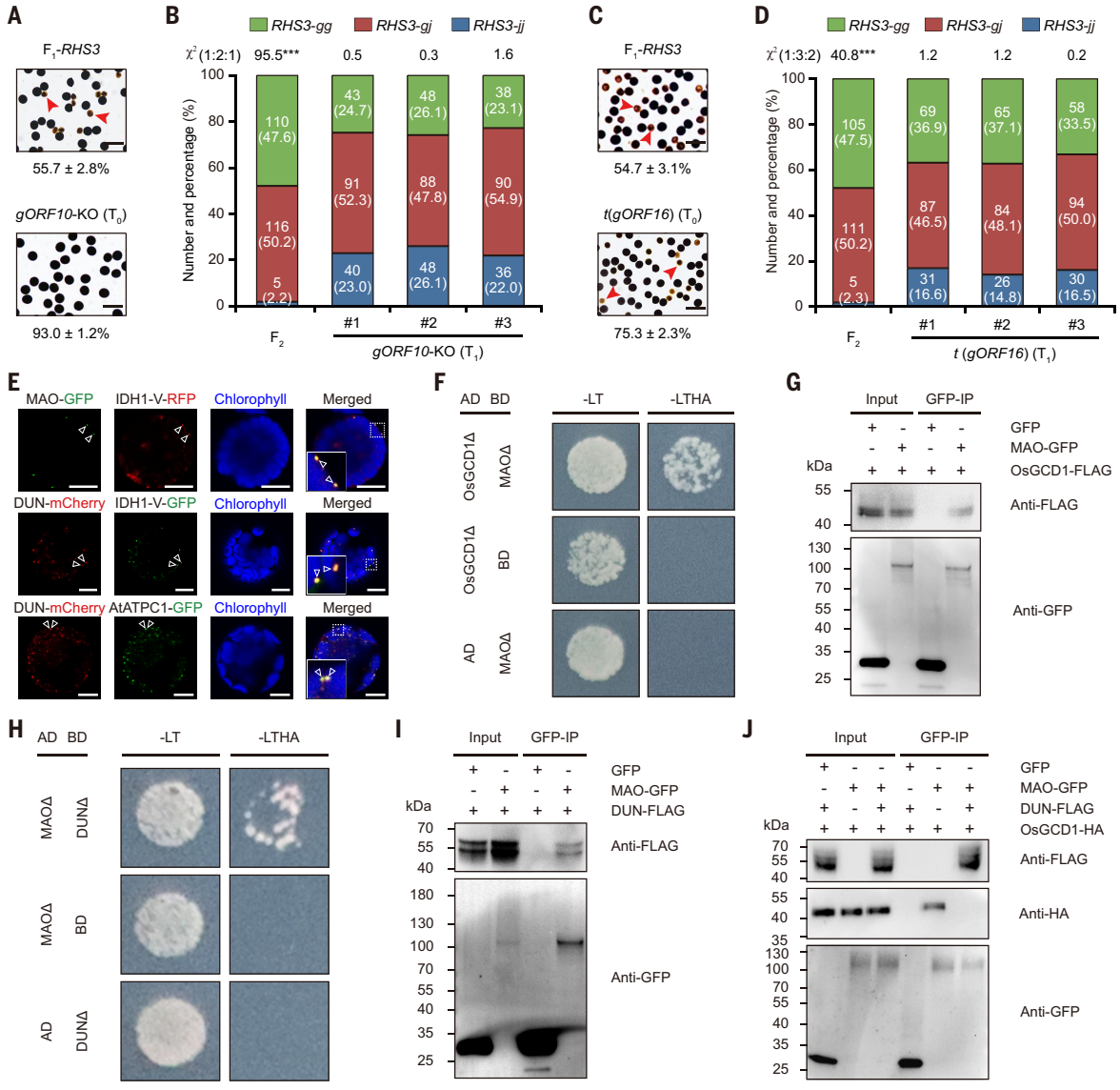

Fig. 2. MAO and DUN act as a toxin–antidote system mediating pollen semisterility. (**A**) Knockout of *gORF10* restores pollen fertility in F_1-*RHS3* plants. Data are means ± SD ($n = 5$ independent florets). Scale bars, 100 μm. (**B**) Segregation of *RHS3* genotypes in progeny (T_1) from selfed *gORF10* knockout F_1-*RHS3* plants follows a 1:2:1 ratio. Asterisks indicate statistically significant differences (χ^2 test, ***$P < 0.001$). (**C**) Introduction of a single-copy *gORF16* transgene partially rescues pollen fertility in F_1-*RHS3*. Data shown as means ± SD ($n = 5$ independent florets). Red arrowheads indicate aborted pollen grains. Scale bars, 100 μm. (**D**) Insertion of a single-copy *gORF16* transgene into F_1-*RHS3* restores the *RHS3* genotypic segregation ratio to 1:3:2 (*jj*:*gj*:*gg*) in T_1 progeny. Asterisks indicate statistically significant differences (χ^2 test, ***$P < 0.001$). (**E**) Subcellular localization of MAO–GFP and DUN–mCherry in protoplasts. MAO–GFP and DUN–mCherry colocalize with IDH1-V, a mitochondrial marker; DUN–mCherry also colocalizes with AtATPC1, a chloroplast marker. Scale bars, 5 μm. (**F**) Yeast two-hybrid (Y2H) assay shows an interaction between MAO and OsGCD1. MAOΔ represents a truncated version lacking the mitochondrial targeting signal. (**G**) Coimmunoprecipitation (Co-IP) assay confirms interaction between MAO and OsGCD1 in rice protoplasts. OsGCD1–FLAG is coprecipitated by MAO–GFP. (**H**) Y2H assay shows an interaction between MAO and DUN. DUNΔ represents a truncated version lacking the mitochondrial targeting signal. (**I**) Co-IP assay confirms interaction between MAO and DUN in rice protoplasts. DUN–FLAG is coprecipitated by MAO–GFP. (**J**) Co-IP assay demonstrates that DUN–FLAG disrupts the interaction between MAO–GFP and OsGCD1–HA.

indicating selective elimination of transgene-free male gametes. These results establish *MAO* and *DUN* as a toxin–antidote pair underlying *RHS3*-mediated pollen semisterility.

DUN binds to MAO to protect mitochondria

To investigate how the *MAO–DUN* element regulates hybrid sterility, we first examined the expression patterns of *MAO* and *DUN*. Both genes were weakly expressed in vegetative tissues. *MAO* accumulated mainly in developing anthers and pistils, whereas *DUN* was most abundant in anthers (fig. S5, A and B). Consistent with predicted targeting sequences, MAO localized exclusively to mitochondria, whereas DUN localized to both mitochondria and chloroplasts (Fig. 2E, and fig. S5, C and D).

A yeast two-hybrid (Y2H) screen identified seven candidate MAO-interacting proteins (fig. S5E), among which OsGCD1 was of particular interest because of its essential role in gamete development (*29*, *30*). Consistent with previous reports, homozygous *Osgcd1* mutants were not recovered. Heterozygous plants (*OsGCD1*-He) showed pollen and spikelet semisterility together with defective embryo sac development (fig. S6, A to F). Reciprocal crosses between *OsGCD1*-He and wild-type (WT)

DJY1 yielded exclusively WT progeny, indicating complete failure of *Osgcd1* transmission through both male and female gametes (fig. S6G). OsGCD1 protein self-interacted in coimmunoprecipitation (co-IP) and bimolecular fluorescence complementation (BiFC) assays, indicating that it forms homo-oligomers (fig. S6, H and I). OsGCD1 colocalized and interacted with MAO in mitochondria, as demonstrated by Y2H, BiFC, and co-IP assays (Fig. 2, F and G, and fig. S7, A and B). MAO disrupted OsGCD1 homo-oligomerization (fig. S7C), suggesting that it induces mitochondrial toxicity by impairing OsGCD1 function.

DUN directly interacted with MAO, as demonstrated by Y2H, BiFC, and co-IP assays (Fig. 2, H and I, and fig. S7D), and these two proteins colocalized in mitochondria (fig. S7E). Although DUN did not affect the mitochondrial colocalization of MAO and OsGCD1, it competed with OsGCD1 for MAO binding (Fig. 2J and fig. S7E), thereby relieving MAO-mediated inhibition of OsGCD1 function. These findings suggest that DUN neutralizes MAO toxicity by sequestering MAO and preserving OsGCD1 function.

JIA specifically protects female gametes

Most so far characterized rice hybrid sterility loci affect either pollen or embryo sac fertility (*17*, *31*). Unexpectedly, knocking out *gORF4* in F_1-*RHS3* plants reduced spikelet fertility to approximately 50% without affecting pollen fertility (Fig. 3, A and B, and fig. S8A), suggesting a role in female gamete transmission. Because the *RHS3-j* allele contains *ORF4* (Fig. 1C), disruption of *jORF4* in the same background produced a phenotype indistinguishable from that of *gORF4* mutants (Fig. 3, A and B, and fig. S8A). Genotyping of T_1 progeny derived from selfed T_0 *ORF4* knockout plants revealed that nearly all progeny carried only the *RHS3-gg* allele when *jORF4* was knocked out, whereas progeny from *gORF4* knockout plants were almost exclusively heterozygous (*RHS3-gj*) (Fig. 3C and fig. S8, B and C), indicating that female gametes lacking functional *jORF4* or *gORF4* were not transmitted. Together, these findings suggest that both *gORF4* and *jORF4* function as female gamete–specific antidotes. We therefore designated *ORF4* as *JIA*, meaning "armor" in Chinese.

To validate the antidote function of *JIA*, we generated heterozygous *gJIA/gjia* and homozygous *gjia/gjia* mutants in the NIL-*RHS3* background. The *gJIA/gjia* and *gjia/gjia* plants showed spikelet semisterility and near-complete sterility, respectively, while retaining normal pollen fertility (Fig. 3, D and E, and fig. S8D). At anthesis, mature embryo sacs of *gjia/gjia* plants were completely devoid of nuclei, in contrast to the characteristic eight-nucleate structure of WT embryo sacs (fig. S8E). Only *gJIA*/*gJIA* and *gJIA*/*gjia* genotypes were recovered among T_1 progeny from selfed *gJIA/gjia* plants, segregating at an approximately 1:1 ratio (Fig. 3F and fig. S8F), indicating that female gametes lacking functional *gJIA* were not transmitted. Moreover, simultaneous knocking out of *MAO* and *gJIA* in the NIL-*RHS3* background restored spikelet fertility to near WT levels (Fig. 3, E and F). Collectively, these results demonstrate that *MAO* exerts cytotoxic effects on both pollen and female gametes, whereas *JIA* protects female gametes by neutralizing *MAO* toxicity.

Because *DUN* protects pollen from *MAO* toxicity, we further investigated whether it also protects female gametes. Heterozygous *DUN*/*dun* plants generated by gene editing in the NIL-*RHS3* background showed semisterility in both pollen and spikelets (fig. S8, G to I, and data S6). Consistent with this, approximately 50% of the embryo sacs were aborted (fig. S8, J and K). In the genotyped T_1 progeny, no *dun*/*dun* homozygotes were detected (fig. S8, L and M), indicating that *DUN* protects both male and female gametes from *MAO* toxicity, whereas *JIA* provides an additional, female-specific protective role.

JIA cooperates with DUN to detoxify MAO

We next investigated how JIA specifically protects female gametes. In F_1-*RHS3* plants, *JIA* expression was highest in developing anthers, followed by developing pistils (fig. S9A). The *gJIA* and *jJIA* alleles were expressed at comparable levels (fig. S9B). The encoded proteins differ by only eight amino acid substitutions and both contain a predicted chloroplast transit peptide and an anthranilate phosphoribosyltransferase domain (fig. S10, A and B). Both gJIA and jJIA showed a dual localization to chloroplasts and autophagosomes (Fig. 4, A and B, and fig. S10, C to J). Immunogold labeling in DJY1 root tip cells further confirmed the localization of jJIA to plastids and autophagosomes (fig. S11). These observations suggest that JIA may detoxify MAO by targeting it for autophagic degradation.

We next performed interaction assays and found that both gJIA and jJIA interacted with DUN, but not with MAO (figs. S12 and S13, A and B). However, both MAO–FLAG and DUN–FLAG were coimmunoprecipitated with JIA–GFP (fig. S13, C and D), indicative of the formation of a JIA–DUN–MAO tripartite complex. Coexpression of JIA and DUN in protoplasts redirected DUN–GFP from mitochondria and chloroplasts to autophagosomes (Fig. 4C and fig. S14, A and B). Likewise, coexpression of MAO with JIA and DUN redirected MAO–GFP to autophagosomes (Fig. 4D and fig. S14, C and D). These findings suggest that JIA uses DUN as a molecular bridge to recruit MAO into a JIA–DUN–MAO complex and target it to autophagosomes for degradation.

Selective autophagy receptors recruit cargo proteins to autophagosomes by interacting with ATG8 through ATG8-interacting motifs (AIMs) (*32*). Because the rice genome encodes seven ATG8 isoforms (*33*), we tested whether JIA interacts with any of them. Both gJIA and jJIA interacted specifically with OsATG8e in yeast, which was further validated by co-IP and BiFC assays (fig. S15). In silico analysis identified seven putative AIMs (AIM1–7) in JIA. To determine which motif mediates OsATG8e binding, we individually mutated each AIM and reassessed the interaction. Disruption of AIM3 alone abolished the JIA–OsATG8e interaction in yeast (fig. S16, A and B). Notably, loss of this interaction disrupted the autophagosomal localization of JIA while retaining its chloroplast localization in protoplasts (fig. S16, C and D).

To test the in vivo function of AIM3, we mutated this motif in the NIL-*RHS3* background. Heterozygous *AIM3/aim3* plants showed normal pollen fertility but approximately 50% spikelet fertility, and *AIM3/AIM3* and *AIM3/aim3* genotypes segregated at a 1:1 ratio in the T_1 generation (fig. S16, E to G), indicating selective elimination of female gametes carrying the *aim3* allele. We further performed a semi–in vivo degradation assay by incubating purified MBP–MAO with total protein extracts from young panicles. MAO was degraded by extracts from NIL-*RHS3* plants harboring functional *gJIA*, but not by extracts from *gJIA* knockout plants, and this degradation was blocked by the autophagy inhibitor Bafilomycin A1 (Fig. 4E). Together, these findings establish JIA as a selective autophagy receptor that recruits the JIA–DUN–MAO complex to autophagosomes for degradation.

Evolutionary trajectory of *RHS3*

BLAST analysis showed that *JIA* is restricted to a subset of Poaceae species (fig. S17A), whereas *MAO* and *DUN* are restricted to the genus *Oryza*. JIA proteins from multiple *Oryza* species, including AA- and BB-genome wild rice and AA-genome cultivated rice, retained an intact AIM3 motif and interacted with OsATG8e in yeast (fig. S17B). By contrast, JIA homologs from *Triticum aestivum*, *Sorghum bicolor*, and *Zea mays* failed to interact with OsATG8e as a result of the replacement of the conserved AIM3 Ile residue with Val or Lys (fig. S17, A and B), indicating that the protective function of JIA is restricted to *Oryza*.

To investigate the origin of the 94.3-kb SV encompassing *MAO* and *DUN*, we analyzed chromosome-level genome assemblies from five AA-genome wild species (*O. meridionalis*, *O. longistaminata*, *O. glumaepatula*, *O. barthii*, and *O. rufipogon*), one BB-genome species (*O. punctata*), and two CC-genome species (*O. officinalis* and *O. eichingeri*). Synteny analysis showed that *MAO* and *DUN* are present exclusively in AA-genome species and absent from BB- and CC-genome wild rice (Fig. 4F and data S7), indicating an origin within

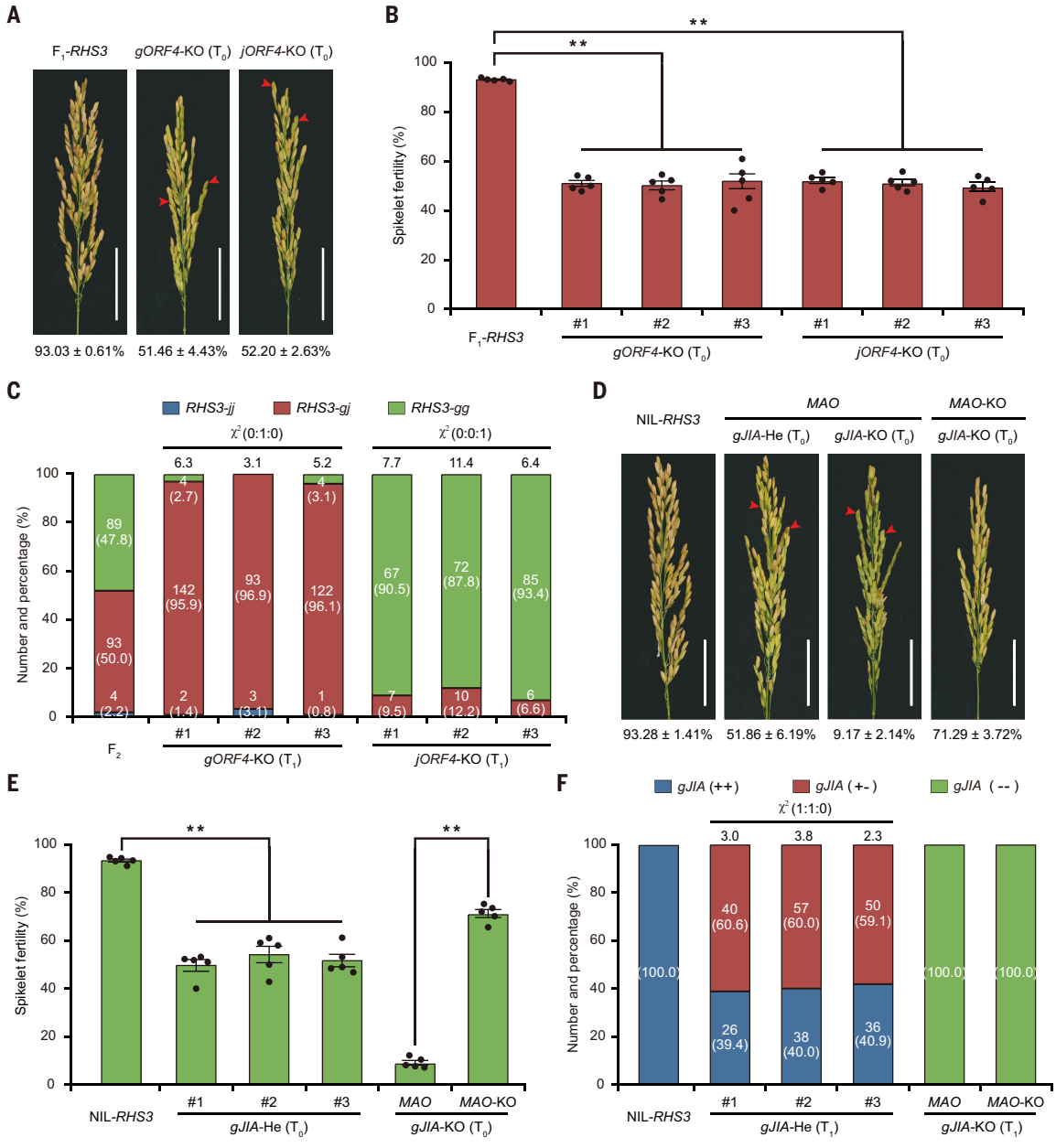

Fig. 3. *JIA* protects female gametes by detoxifying *MAO*. (**A**) Knockout of either *gORF4* or *jORF4* in F_1-*RHS3* plants leads to spikelet semisterility. Red arrowheads indicate shriveled grains. Data shown as means ± SD ($n = 5$ independent panicles). Scale bars, 10 cm. (**B**) Quantification of spikelet fertility in F_1-*RHS3*, *gORF4*-knockout, and *jORF4*-knockout lines. Data shown as means ± SD ($n = 5$ independent panicles). Asterisks indicate statistically significant differences (Student's *t*-test, $^{**}P < 0.01$). (**C**) Genotypic segregation of *RHS3* following *gORF4* and *jORF4* knockout in F_1-*RHS3*. A 0:1:0 (*jj*:*gj*:*gg*) ratio is observed for *gORF4* knockout, and a 0:0:1 (*jj*:*gj*:*gg*) ratio for *jORF4* knockout. (**D**) Knocking out of *gJIA* almost abolishes spikelet fertility in the NIL-*RHS3* background but the reduced fertility is largely restored when *MAO* is knocked out. Red arrowheads indicate shriveled grains. Data shown as means ± SD ($n = 5$ independent panicles). Scale bars, 10 cm. (**E**) Quantification of spikelet fertility in control, heterozygotes and homozygous *gJIA* mutants, and *gJIA*/*MAO* double-knockout lines. Data shown as means ± SD ($n = 5$ independent panicles). Asterisks indicate statistically significant differences (Student's *t*-test, $^{**}P < 0.01$). (**F**) Genotypic segregation of *gJIA* in selfed progeny of heterozygous mutant shows a 1:1:0 (++:±:−−) ratio.

the AA-genome lineage. Using the conserved flanking genes *ORF9* and *ORF17*, we extracted the *ORF9–17* interval for comparative analysis. Only *O. barthii*, the wild progenitor of *O. glaberrima*, contains an intact 94.3-kb SV, whereas other wild species either lack it or harbor only partial segments. The SV could be resolved into a 48.7-kb left segment (L-SV; *gORF10–13*) and a 45.6-kb right segment (R-SV; *gORF14–16*). The L-SV and R-SV show highest homology to the corresponding regions in *O. glumaepatula* and *O. meridionalis*, respectively (Fig. 4G), suggesting that the 94.3-kb SV in *O. barthii* has a composite origin involving these two species. *O. rufipogon* contains three SV types in this region, likely derived from multiple ancestral lineages, including *O. longistaminata*, *O. meridionalis*, and *O. glumaepatula* (fig. S17C).

To assess *MAO* and *DUN* diversity, we analyzed 591 accessions of *O. barthii*, *O. rufipogon*, and cultivated rice from Africa and Asia (data S7). Three *MAO* allele types were identified: functional *MAO*, $MAO^{T/S}$ (alleles carrying premature stop codons or amino acid substitutions predicted to abolish function in the absence of *DUN*), and MAO^{U} (alleles of unknown function). *DUN* alleles were similarly classified into functional *DUN*, DUN^{T} (alleles carrying premature stop codons), and

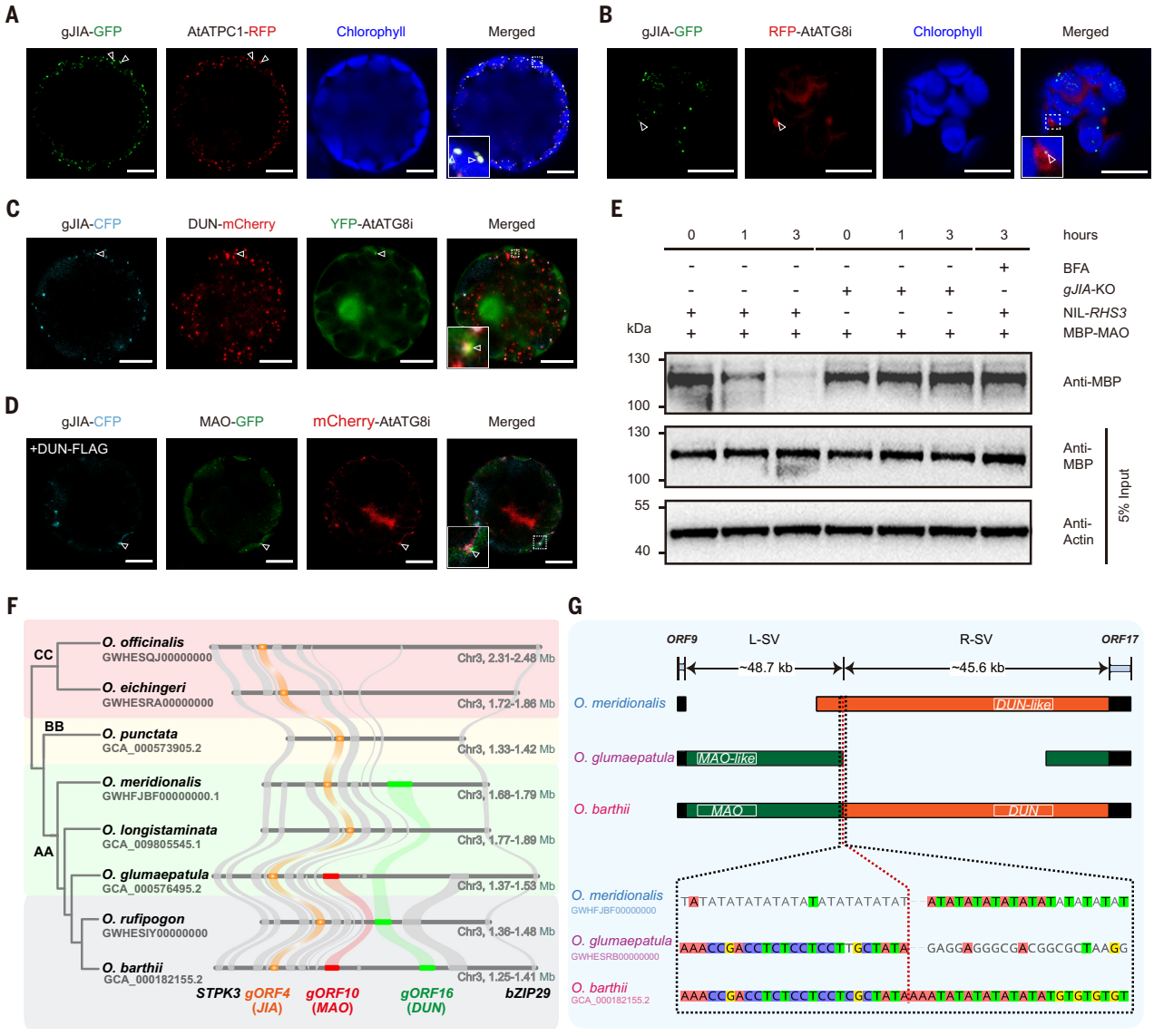

Fig. 4. JIA-mediated detoxification and evolutionary trajectory of the *RHS3* locus. (**A**) Subcellular localization of gJIA–GFP in protoplasts shows colocalization with AtATPC1, a chloroplast marker. Scale bars, 5 μm. (**B**) gJIA–GFP colocalizes with mCherry–AtATG8i, an autophagosome marker. Scale bars, 5 μm. (**C**) DUN colocalizes with gJIA–GFP in autophagosomes upon coexpression. Scale bars, 5 μm. (**D**) Coexpression of gJIA–CFP and DUN–FLAG redistributes MAO–GFP to autophagosomes. Scale bars, 5 μm. (**E**) Semi–in vivo degradation assay of MAO. Purified MBP–MAO is incubated with total protein extracts from young panicles of NIL-*RHS3* or *gJIA* knockout plants. Bafilomycin A1 (BFA) is an inhibitor of autophagic flux. (**F**) Synteny analysis of the *RHS3* locus across representative *Oryza* species arranged according to previously reported whole-genome phylogenetic relationships (corresponding accessions are listed below). *JIA* is evolutionarily conserved across the *Oryza* genus, while *MAO* and *DUN* likely originated de novo in *O. glumaepatula* and *O. meridionalis*, respectively. (**G**) Structural variations at the *RHS3* locus spanning *ORF9* to *ORF17* among representative AA-genome rice species, including *O. meridionalis*, *O. glumaepatula*, and *O. barthii*. Colored boxes above indicate the predicted *ORFs*. Colored segments show the Identity by Descent regions through recombination. The lower panel shows nucleotide sequences at the recombination breakpoint (indicated by red dashed line). Accession identifiers for each species are shown below the corresponding species names. L-SV, left fragment of the SV; R-SV, right fragment of the SV.

DUN^{S} (alleles carrying conserved amino acid substitutions) (data S8 and S9). To assess the functionality of *DUN*^{S}, we introduced a recombinant *DUN*^{S} allele carrying four conserved amino acid substitutions, driven by the native *DUN* promoter, into F_1-*RHS3* plants. T_0 transformants showed pollen semisterility, and *RHS3* genotypes (*jj:gj:gg*) segregated in a 0:1:1 ratio in selfed progeny (fig. S18, A and B), indicating that *DUN*^{S} is nonfunctional. On the basis of the presence and functional status of *MAO* and *DUN*, *MAO–DUN* haplotypes were grouped into seven types: Type I lacks both genes (e.g., DJY1), whereas Type VII carries functional *MAO* and *DUN* (e.g., IRGC 102295). Type II and Type III contain only nonfunctional *DUN* or *MAO*, respectively, while Type IV contains nonfunctional alleles of both genes. Type VI carries functional *DUN*, whereas the functional status of *MAO* remains undetermined. Notably, Type V harbors functional *DUN* but nonfunctional *MAO* (data S10), suggesting a potential wide-compatibility type. This speculation was validated by genetic analyses (fig. S18, C and D).

We next surveyed *MAO–DUN* haplotypes in 672 accessions of AA-, BB- and CC-genome wild rice species. All nine *O. longistaminata* accessions carried Type I. Among 32 *O. meridionalis* accessions, 25 harbored Type I and seven Type II. In *O. glumaepatula*, 11 out of 29 accessions harbored Type I and 18 carried Type III. *O. rufipogon* displayed greater diversity, with Type I predominating (101/158 of accessions), followed

by Type II (49/158) and Type III (8/158). In *O. barthii*, four haplotypes were detected: Type IV (37/101), Type V (2/101), Type VI (3/101) and Type VII (59/101) (fig. S18E). Comparative sequence and phylogenetic analyses suggest that nonfunctional *MAO-like* and *DUN-like* sequences originated de novo in *O. glumaepatula* and *O. meridionalis*, respectively, and were subsequently brought together through introgression or recombination in an unknown intermediate ancestor to form a complete but nonfunctional *MAO–DUN* element. In *O. barthii*, multiple coding sequence mutations rendered both *MAO* and *DUN* functional, a process that accompanied the emergence of reproductive isolation between Asian and African rice lineages. All surveyed *O. rufipogon* and Asian cultivated rice accessions carried nonfunctional *RHS3* haplotypes, whereas functional *RHS3* occurred in 58% of *O. barthii* and 97% of African cultivated rice accessions (fig. S18E), identifying *RHS3* as a major reproductive barrier between Asian and African rice lineages.

Discussion

Here we show that *RHS3* encodes a noncanonical tripartite toxin–antidote system in which *MAO* acts sporophytically to kill both male and female gametes by impairing *OsGCD1*, whereas *DUN* functions gametophytically to rescue *DUN*-carrying male gametes by disrupting the MAO–OsGCD1 interaction (fig. S19). Unlike previously characterized two-component toxin–antidote systems underlying hybrid sterility in rice (*17*, *31*), *RHS3* contains a third component, *JIA*, which acts as a female gamete–specific protector. Mechanistically, JIA interacts with DUN to form a JIA–DUN–MAO complex and binds ATG8e through its AIM3 motif, thereby targeting MAO for autophagic degradation (fig. S19B). These findings identify JIA as a plant-specific selective autophagy receptor that mediates autophagic degradation of MAO, thereby revealing a previously unrecognized mechanism of reproductive isolation in plants.

JIA exerts its protective function only in the presence of the *MAO–DUN* element, suggesting that it represents a cryptic genetic component of the hybrid sterility system. This observation raises the possibility that similar hidden components could be widespread yet remain undetected in conventional genetic analyses, particularly when shared by both parental lineages. The recruitment of *JIA* may also confer evolutionary advantages to the *RHS3* locus. By coopting *JIA*, a gene conserved across *Oryza* species, *RHS3* may circumvent the need to evolve a dedicated antidote. Moreover, although *MAO* impairs both male and female gametes, the conserved function of *JIA* and its female gamete–specific protective activity may allow *RHS3* to increase its transmission without compromising spikelet fertility.

Meeting future rice demand will require sustained increase in productivity under growing population pressure and climate change (*34*, *35*). Interspecific heterosis between Asian and African cultivated rice, exemplified by the successful development of New Rice for Africa (NERICA) varieties, offers considerable potential for further yield improvement (*9*, *10*, *36*). We identified wide-compatibility types of *RHS3* carrying a nonfunctional *MAO* but functional antidote components, which restore fertility when crossed with either Asian or African cultivated rice. These variations provide valuable genetic resources for overcoming interspecific hybrid sterility and advancing Asian–African hybrid rice breeding.

REFERENCES AND NOTES

1. H. U. A. Rezvi *et al.*, *Food Energy Secur.* **12**, e430 (2023).
2. K. De Vos *et al.*, *Nat. Food* **4**, 518–527 (2023).
3. D. Guo *et al.*, *Nature* **642**, 662–671 (2025).
4. C. Y. Jing *et al.*, *Nat. Plants* **9**, 1221–1235 (2023).
5. M. Wang *et al.*, *Nat. Genet.* **46**, 982–988 (2014).
6. J. Y. Choi *et al.*, *PLOS Genet.* **15**, e1007414 (2019).
7. D. Zeng *et al.*, *Nat. Plants* **3**, 17031 (2017).
8. P. W. Wambugu, M. N. Ndjiondjop, R. Henry, *Plants* **8**, 376 (2019).
9. M. P. Jones, M. Dingkuhn, G. K. Aluko, M. Semon, *Euphytica* **92**, 237–246 (1997).
10. Y. Sun *et al.*, *Crop Sci.* **60**, 2343–2353 (2020).
11. J. Li *et al.*, *Sci. Rep.* **13**, 23057 (2023).
12. Y. Koide *et al.*, *Proc. Natl. Acad. Sci. U.S.A.* **115**, E1955–E1962 (2018).
13. Y. Xie *et al.*, *Nat. Commun.* **10**, 2501 (2019).
14. M. A. Bravo Núñez, N. L. Nuckolls, S. E. Zanders, *Trends Genet.* **34**, 424–433 (2018).
15. A. Burga, E. Ben-David, L. Kruglyak, *Annu. Rev. Genet.* **54**, 387–415 (2020).
16. A. L. Sweigart, Y. Brandvain, L. Fishman, *Trends Genet.* **35**, 245–252 (2019).
17. C. Wang, X. Yu, J. Wang, Z. Zhao, J. Wan, *J. Genet. Genomics* **51**, 583–593 (2024).
18. A. Ricou *et al.*, *PLOS Genet.* **21**, e1011451 (2025).
19. J. Yang *et al.*, *Science* **337**, 1336–1340 (2012).
20. X. Yu *et al.*, *Science* **360**, 1130–1132 (2018).
21. C. Wang *et al.*, *Cell* **186**, 3577–3592.e18 (2023).
22. E. Ben-David, A. Burga, L. Kruglyak, *Science* **356**, 1051–1055 (2017).
23. B. G. Herrmann, B. Koschorz, K. Wertz, K. J. McLaughlin, A. Kispert, *Nature* **402**, 141–146 (1999).
24. J. H. Werren, *Proc. Natl. Acad. Sci. U.S.A.* **108**, 10863–10870 (2011).
25. S. Maheshwari, D. A. Barbash, *Annu. Rev. Genet.* **45**, 331–355 (2011).
26. M. E. Frayer, N. V. Robles, M. J. Rodríguez-Barrera, J. M. Coughlan, M. Schumer, *Trends Genet.* **41**, 1068–1095 (2025).
27. Y. Zhang *et al.*, *Mol. Breed.* **28**, 323–334 (2011).
28. Y. Yang *et al.*, *Rice (N. Y.)* **18**, 43 (2025).
29. X. Huang, X. Peng, M. X. Sun, *New Phytol.* **215**, 1039–1058 (2017).
30. J. J. Wu *et al.*, *Dev. Cell* **23**, 1043–1058 (2012).
31. Y. Ouyang, Q. Zhang, *Annu. Rev. Plant Biol.* **64**, 111–135 (2013).
32. V. V. Rogov *et al.*, *Autophagy Rep.* **2**, 2188523 (2023).
33. K. Xia *et al.*, *DNA Res.* **18**, 363–377 (2011).
34. X. Guo, W. Luo, K. Chong, *Sci. Bull.* **70**, 1364–1367 (2025).
35. J. Y. Li, C. Yang, J. Xu, H. P. Lu, J. X. Liu, *Plant Cell Environ.* **46**, 1087–1103 (2023).
36. O. F. Linares, *Proc. Natl. Acad. Sci. U.S.A.* **99**, 16360–16365 (2002).
37. K. Zhao, Code for: A tripartite genetic conflict system controls hybrid sterility in rice, Zenodo (2026); https://doi.org/10.5281/zenodo.20579119.

ACKNOWLEDGMENTS

We thank X. Wei, L. Zhang, L. Zhou, X. Yang, and T. Yu for assistance with rice field management and hybridization; Q. Yang and Y. Cheng for providing wild rice accessions; X. Ma for sharing rice landrace resources; and K. Olsen for critical reading of the manuscript and valuable discussions. **Funding:** This study was supported by the Scientific Research Innovation Capability Support Project for Young Faculty (ZYGXQNJSKYCXNLZCXM-A7), the National Key Research and Development Program of China (2022YFD1200801 and 2022YFF1003503), the National Natural Science Foundation of China (32422067), the Jiangsu Province Natural Science Foundation (BK20240089), and the Key Project for Zhongshan Biological Breeding Laboratory (ZSBBL-KY2023-04 and ZSBBL-KY2023-07). C.Wang acknowledges support from the 2024 DAMO Academy Young Fellow Award. Additional support was provided by the Key Laboratory of Biology, Genetics and Breeding of Japonica Rice in the Mid-lower Yangtze River and the Jiangsu Collaborative Innovation Center for Modern Crop Production. **Author contributions:** X.H. and K.S. performed most of the experiments and analyzed the data. Ying Zhu and Y. Zeng performed subcellular location and immunogold labeling assays. Y.X. performed protein purification assays. Jing Li, Y. Zhang, C.L., X. Dong, Y.R., J. Wang, Y.H., S. Cheng, B.Y., T.S., J.X., Jiayu Lu, D.L., A.J., J.G., S. Cui, G.X., X.L., Y.T., S.L., X. Deng, J.Z., D.T., J.T., and L.C. developed materials and performed genetic analysis. K.Z., X.Z., Hongru Wang, X. Gan, Y.Y., S.G., Yuantao Zhu, L.H. and C.X. performed the evolutionary analysis. X. Guo and L.J. performed the genetic transformation. J.T., Letian Chen and X.Y. discussed the manuscript. C. Wang, Haiyang Wang, C. Wu, Z.Z. and J. Wan wrote the manuscript. J.Wan conceived and supervised the project. **Competing interests:** J. Wan, X.H., C. Wang, K.S., Z.Z., L.J., X.Y., X.L., S.L., Y.T. and Liangming Chen are inventors on a pending patent (202410734804.8) in China related to this work. The other authors declare no competing interests. **Data, code, and materials availability:** The sequences of *MAO*, *DUN*, *gJIA* and *jJIA* have been deposited in GenBank under accession numbers PV833341–PV833344. The raw sequencing data, including transcriptome data from IRGC 102295 young panicles at the meiosis stage and its whole-genome sequence, have been deposited in the NCBI Sequence Read Archive under BioProject accession PRJNA1426876. All other data needed to evaluate the conclusions in the paper are available in the main text, supplementary material or data S1 to S11. Original uncropped gel blot images are provided in data S1 and S2. The custom code used for the genomic and phylogenetic analyses of the *RHS3* locus has been deposited at Zenodo (*37*). All materials generated in this manuscript will be made available upon request to J. Wan under a material transfer agreement.

SUPPLEMENTARY MATERIALS

science.org/doi/10.1126/science.aec5252
Materials and Methods; Figs. S1 to S19; References (*38*–*44*); MDAR Reproducibility Checklist; Data S1 to S11

Submitted 23 September 2025; resubmitted 1 May 2026; accepted 3 July 2026

10.1126/science.aec5252

A tripartite genetic conflict system controls hybrid sterility in rice

Xiaodong He, Zhigang Zhao, Kun Shao, Xiaowen Yu, Ying Zhu, Jintao Tang, Jing Li, Yunhui Zhang, Keyu Zhao, Xiaoming Zheng, Hongru Wang, Chao Li, Xiangchao Gan, Xiaoou Dong, Yulong Ren, Yehui Xiong, Jian Wang, Yang Hu, Siqi Cheng, Bowen Yao, Yulu Ye, Song Guo, Yuantao Zhu, Ling He, Tiaofeng Shan, Chen Xu, Jinxuan Xu, Jiayu Lu, Dekun Lei, Anqi Jian, Junwen Gao, Song Cui, Gencheng Xu, Xiuping Guo, Xi Liu, Yunlu Tian, Shijia Liu, Ling Jiang, Xianneng Deng, Jiawu Zhou, Dayun Tao, Yonglun Zeng, Letian Chen, Chuanyin Wu, Haiyang Wang, Chaolong Wang, and Jianmin Wan

Science **393** (6814), . DOI: 10.1126/science.aec5252

Editor's summary

Asian and African rice are the only two domesticated rice species. Asian-African hybrid rice offers a path to higher yield and resilience but faces hybrid sterility barriers. Using genome-wide linkage analysis, He *et al*. identified *RHS3* as the quantitative trait locus underlying this incompatibility. *RHS3* consists of three genes, *MAO*, *DUN*, and *JIA*. MAO functions as a toxin affecting both male and female gametes. In pollens, DUN functions as an antidote competitively inhibiting MAO's toxicity, whereas in female gametes, JIA and DUN together target MAO for detoxification through autophagy. The researchers found rice lines with functional antidote DUN but nonfunctional toxin MAO, providing a potential resource for Asian-African hybrid rice breeding. —Unnati Sonawala and Madeleine Seale